HHS Public Access

Author manuscript

Nat Neurosci. Author manuscript; available in PMC 2013 March 01.

Published in final edited form as:

Nat Neurosci. 2012 September ; 15(9): 1195–1197. doi:10.1038/nn.3162.

Co-activation of multiple tightly-coupled calcium channels triggers spontaneous release of GABA

Courtney Williams[1], **Wenyan Chen**[1], **Chia-Hsueh Lee**, **Daniel Yaeger**, **Nicholas P. Vyleta**[2], and **Stephen M. Smith**[3]

Division of Pulmonary & Critical Care Medicine, Oregon Health & Science University, Portland, OR 97239

Abstract

Voltage-activated Ca^{2+} channels (VACCs) mediate Ca^{2+} influx to trigger action potential-evoked neurotransmitter release but the mechanism by which Ca^{2+} regulates spontaneous transmission is unclear. Here we show VACCs are the major physiological triggers for spontaneous release at murine neocortical inhibitory synapses. Moreover, despite the absence of a synchronizing action potential, we find that spontaneous fusion of a GABA-containing vesicle requires the activation of multiple tightly-coupled VACCs of variable type.

Spontaneous and evoked neurotransmission, two forms of interneuronal communication, have been proposed to rely on different signaling mechanisms[1] and to mediate physiologically distinct functions[2]. While it is well-established that presynaptic action potentials activate VACCs, triggering Ca^{2+} influx and synchronous release of neurotransmitter, how external $[Ca^{2+}]$ ($[Ca^{2+}]_o$) is coupled to spontaneous release remains controversial. Although increasing $[Ca^{2+}]_o$ enhances spontaneous neurotransmission at excitatory neocortical synapses, blocking of VACCs or buffering of intracellular $[Ca^{2+}]$ ($[Ca^{2+}]_i$) has no effect on spontaneous release[3]. In contrast, at GABAergic cortical synapses mutation of Ca^{2+}-sensors, such as synaptotagmin-1, impacts spontaneous release, suggesting a major role for Ca^{2+} influx[4]. Here we show that, in contrast to regulation of excitatory synapses, spontaneous release from inhibitory synapses is dependent on VACCs and that single vesicle fusion requires coincident activation of multiple closely packed VACCs.

[3]Correspondence should be addressed to: Dr. Stephen M. Smith, Division of Pulmonary & Critical Care Medicine, 3181, SW Sam Jackson Park Road, UHN-67, O.H.S.U., Portland, OR 97239, USA., Telephone: (503)494-2736, Fax: (503)494-7368, smisteph@ohsu.edu.

[1]these authors contributed equally.

[2]Current address: Institute of Science and Technology, Austria.

Author Contributions

CW conducted the calcium chelation, specific toxin- block of mIPSC and VACC currents, and VACC gating experiments and participated in writing the manuscript. WYC conducted the calcium chelation, Cd^{2+} and specific toxin- block of mIPSC and VACC currents, and hyperpolarization experiments. CHL conducted the calcium concentration-effect experiments. DY conducted the Cd^{2+} block of mIPSC and hyperpolarization experiments. NPV provided cell cultures and participated in writing the manuscript. SMS designed experiments, analyzed data, and wrote the manuscript.

We examined how $[Ca^{2+}]_o$ is coupled to spontaneous release of GABA by recording miniature inhibitory postsynaptic currents (mIPSCs) in cultured neocortical neurons. Changing $[Ca^{2+}]_o$ from 1.1 mM, altered mIPSC frequency in a reversible and concentration-dependent manner (Fig. 1a-c, n=6). The steepness of the concentration-effect relationship was much lower (slope=0.45) compared to evoked release[5] but similar to that for mEPSCs[3]. Application of Cd^{2+} (100 μM), a VACC blocker, reduced mIPSC frequency by 56±7% (n=6) from the basal level when $[Ca^{2+}]_o$ was 1.1 mM (Fig. 1d). At 6 mM Ca^{2+} mIPSC frequency was 185±46% above basal level and relatively reduced by 56±8% following Cd^{2+} application. These data indicate VACCs trigger spontaneous GABA release at both physiological and elevated $[Ca^{2+}]_o$. Stochastic VACC activity should be decreased by presynaptic hyperpolarization. Reduction of external $[K^+]$ from 4 to 1 mM, to hyperpolarize the nerve terminals, reversibly reduced mIPSC frequency by 34±8% (SuppFig. 1, n=6) but had little effect when VACC were blocked by Cd^{2+}. These data demonstrate that, in contrast to glutamatergic excitatory synapses[3], VACCs regulate spontaneous GABA release at neocortical synapses.

Evoked GABA release is regulated by VACC subtypes in the order P/Q->N->R-types at cortical synapses[6]. To determine which VACCs regulate spontaneous GABA release, we applied specific channel type blockers while recording mIPSCs. Blockade of N-type channels with a saturating dose[7] of ω-conotoxin-GVIa (GVIa, 1 μM) reduced mIPSC frequency by 32±7% (n=9; Fig.2a,b). Subsequent addition of a saturating concentration[8] of the P/Q-type blocker ω-Aga-toxin-IVa (Aga-IVa, 300 nM) reduced mIPSC frequency by 11±4% suggesting a larger contribution by N- than P/Q-type VACCs (Fig. 2a,b, p=0.015). Cd^{2+} reduced mIPSC frequency a further 23±8% (Fig. 2a,b), indicating contributions by L- or R-type VACCs. On average, 33±6% of mIPSCs were Cd^{2+} resistant suggesting that other regulatory mechanisms also contribute to spontaneous GABA release[3]. Taken together these data indicate that P/Q- and N- type VACCs are important triggers of mIPSCs.

At most synapses the simultaneous activation of multiple VACCs has been implicated as necessary to trigger single vesicle fusion during evoked release whereas it has been proposed that spontaneous release results from the activation of a single VACC[9–11]. If each fusion event depends on the opening of a single channel the impact of the block of P/Q- or N-type VACCs with slowly dissociating toxins will be independent of each other. Conversely, if multiple channels are involved, cooperativity will result in proportionately smaller reductions in release probability as the total fraction of VACC blocked is increased[12]. Consistent with multiple channel involvement, the relative effectiveness of 300 nM Aga-IVa and 1 μM GVIa was reversed when the order of toxin application was switched (32±7% versus 3±3%, p=0.050, Fig. 2c,d). This was not due to interneuronal variability of the proportion of mIPSCs independent of VACCs, as the reversal in the apparent effectiveness of GVIa and Aga-IVa was also evident when we compared the toxin's actions on the Cd^{2+}-sensitive fraction (Fig. 2e). In other words GVIa and Aga-IVa were more effective at reducing mIPSC frequency when the neuron had not already been exposed to saturating doses of the other blocker (p=0.008 and p=0.018 respectively; Fig. 2e). At higher doses Aga-IVa cross-reacts with N-type channels[13]. To test if cross-reactivity was responsible for the reduced effects of the second toxin applications on mIPSC frequency we directly measured VACC current block in these neurons. The percentage of the total VACC

currents carried by 1 μM GVIa- and 300 nM Aga-IVa-sensitive fractions were unchanged by the order of toxin application (Supp. Fig. 2) indicating cross-reactivity was not responsible for the reduced effect of the second toxin application (Fig. 2). Collectively, the data obtained from channel-type specific toxins show that each fusion event was dependent on multiple VACCs *and* that different VACC types cooperate to trigger fusion of a single vesicle.

How close are these VACCs to the vesicle? One hypothesis is that VACCs are not tightly associated with vesicles but cooperate to raise bulk $[Ca^{2+}]_i$ which increases mIPSC frequency. BAPTA and EGTA, have similar affinities for Ca^{2+} but BAPTA has a ~40 times faster rate of binding so that at mM concentrations BAPTA will impact signaling if the mean diffusion distance for Ca^{2+} is as short as 10–20 nm, whereas EGTA will only have an effect if the path length is relatively long (>100 nm)[11]. Application of cell-permeant BAPTA-AM (50 μM) substantially reduced the $[Ca^{2+}]_o$-dependent increase in mIPSC frequency (Fig. 3a,b; p=0.007, n=8;) indicating this Ca^{2+} buffer attenuated the $[Ca^{2+}]_i$ transient when $[Ca^{2+}]_o$ was 6 mM. In contrast, EGTA-AM (50 μM) did not change the response to increases in $[Ca^{2+}]_o$ (Fig. 3a,c, Suppl. Fig. 3; p=0.391, n=6). At physiological $[Ca^{2+}]_o$ BAPTA reduced mIPSC frequency by 24±7% (n=14) while EGTA was ineffective (Fig. 3d,e; 1±6%, n=16; p=0.009). Application of Cd^{2+} after BAPTA exposure reduced mIPSC frequency further (Fig. 3d,f, Suppl. Fig. 3; by 65±7%, n=7). Given that the final intracellular concentrations of the two buffers are likely to have been similar, these combined data strongly indicate that VACCs triggered spontaneous GABA-release via tightly coupled vesicles and not by changing bulk $[Ca^{2+}]_i$ [11, 14]. Interestingly, action potential-evoked release of a single GABA-containing vesicle relies on a vesicle-VACC coupling distance of 10–20 nm and activation of up to three VACCs[10].

An important physiological consequence of the requirement that multiple VACC openings combine to trigger each mIPSC will be a lower basal rate of spontaneous GABA release due to the low probability of coincident VACC openings. The mechanism synchronizing the activation of multiple VACCs remains unclear. Based on somatic VACC currents, stochastic synchronization seems unlikely, although it cannot be ruled out, since the membrane potential (−78±2mV; n=17) sits at the foot of the VACC current activation curve (Suppl. Fig. 4). Another possibility is that nerve terminal VACCs are linked via their C-termini, leading to coupled gating similar to the mechanism proposed to synchronize L-type VACC activity [15]. The importance of VACCs as triggers for spontaneous GABA release is surprising in the light of our earlier findings that spontaneous glutamate release is not initiated by Ca^{2+} influx[3], and indicates a substantial difference between the regulation of GABAergic and glutamatergic synapses in the neocortex. Further research is required to identify the constituents at the active zone responsible for the differential regulation of inhibitory and excitatory spontaneous release and to determine if this phenomenon extends to other regions of the brain.

METHODS

Neuronal cell culture

Neocortical neurons were isolated from postnatal day 1–2 mouse pups as described previously[16]. All animal procedures were approved by Oregon Health & Science

University's Institutional Animal Care and Use Committee in accordance with the U.S. Public Health Service Policy on Humane Care and Use of Laboratory Animals and the National Institutes of Health Guide for the Care and Use of Laboratory Animals. Animals were decapitated following general anesthetic with isoflurane and then the cerebral cortices were removed. Cortices were incubated in trypsin and DNase and then dissociated with a heat polished pipette. Dissociated cells were cultured in MEM plus 5% FBS on glass coverslips. Cytosine arabinoside (4 μM) was added 48 hours after plating to limit glial division. Cells were used after a minimum of 14 days in culture.

Electrophysiological recordings

Cells were visualized with an Olympus IX70 inverted microscope. Recordings were made in whole-cell voltage clamp mode in neurons voltage-clamped at −70 mV. Voltages were corrected for liquid junction potentials[17]. In general and except where stated in the text, extracellular solution contained the following (in mM): 150 NaCl, 4 KCl, 10 HEPES, 10 glucose, 1.1 $MgCl_2$, pH 7.35 with NaOH. $CaCl_2$ was 1.1 mM unless otherwise indicated. Recordings of mIPSCs were made in the presence of tetrodotoxin (TTX; 1 μM) and CNQX (10 μM) to block Na^+ channels and AMPA receptors, respectively. Recordings of mIPSCs were made using a potassium chloride-rich intracellular solution containing the following (in mM): 118 KCl, 9 EGTA, 10 HEPES, 4 $MgCl_2$, 1 $CaCl_2$, 4 NaATP, 0.3 NaGTP, 14 creatinine phosphate, pH 7.2 with KOH. Electrodes had resistances of 3–7 MΩ. VACC currents were isolated using cesium methane-sulfonate rich solution as described previously[3]. Currents were recorded with a HEKA EPC9/2 amplifier and filtered at 1 kHz using a Bessel filter and sampled at 10 kHz. Series Resistance (R_s) was monitored, and recordings were discarded if R_s changed significantly during the course of a recording. R_s was compensated to ~70% in recordings of VACC currents.

Solution Application

Solutions were gravity fed through a glass capillary (1.2 mm outer diameter) placed ~1 mm from the patch pipette tip. Toxin (Alomone Labs) stock solutions were all made at 1000X concentration with distilled water and stored at −20 °C. Cytochrome C (0.1 mg/ml) was also added to Aga-IVa-containing solutions to minimize non-selective toxin binding to the apparatus. BAPTA-AM (Invitrogen) was dissolved in DMSO at 50 mM stock concentration. Before use, extracellular solution was incubated at 30°C while undergoing ultrasonic agitation for ≥30 min to ensure BAPTA-AM dissolved completely. EGTA-AM (Invitrogen) was dissolved in DMSO at 50 mM stock concentration.

Analysis

Data were acquired on a PIII computer and analyzed with IgorPro (Wavemetrics) and Minianalysis (Synaptosoft) software using a threshold crossing algorithm. Miniature IPSC data were normalized to the basal level by dividing the mIPSC frequency measured over each ten second interval by the average mIPSC frequency over 100–200 s at the beginning of the experiment. Steady-state mIPSC frequency changes were the averages measured over ≥60 seconds as a percentage of the basal level. In some experiments (Fig. 2e) reductions in mIPSC frequency were described as a percentage of the Cd^{2+}-sensitive component by comparing the response to blockers as a fraction of the difference between the basal mIPSC

rate and the mIPSC rate following application of Cd^{2+} (100 μM). Exemplar plots of mIPSC frequency versus time are shown as supplementary information (Supp. Fig. 4) to illustrate the variability of basal mIPSC frequency rates which presumably reflect differences in the number of synapses and release probability. The average basal mIPSC frequency was 5.3 ± 0.6 s^{-1}(n= 61).

Statistical Analysis

Data values are reported as mean ± SEM. Pairwise comparison of data were performed using Student's t test or Mann-Whitney U-test if the data were not normally distributed (Microsoft EXCEL or Sigmaplot). We used two-way repeated measures ANOVAs to examine the impact of BAPTA-AM and EGTA-AM on the mIPSC frequency at different external calcium levels. Subsequent pairwise comparisons were performed with the Holm-Sidak method (Sigmaplot). Curve fitting was carried out using IgorPro (Wavemetrics).

Supplementary Material

Refer to Web version on PubMed Central for supplementary material.

Acknowledgments

We thank Drs. Michael Andresen and Kamran Khodakhah for helpful comments. The work was supported by the NIH (DA027110 and GM097433) and OCTRI. CW and NPV were supported by T32HL033808 from the National Heart, Lung, and Blood Institute.

References

1. Sara Y, Virmani T, Deak F, Liu X, Kavalali ET. Neuron. 2005; 45:563–573. [PubMed: 15721242]
2. Autry AE, et al. Nature. 2011; 475:91–95. [PubMed: 21677641]
3. Vyleta NP, Smith SM. J. Neurosci. 2011; 31:4593–4606. [PubMed: 21430159]
4. Xu J, Pang ZP, Shin OH, Sudhof TC. Nat. Neurosci. 2009; 12:759–766. [PubMed: 19412166]
5. Lou X, Scheuss V, Schneggenburger R. Nature. 2005; 435:497–501. [PubMed: 15917809]
6. Cao YQ, Tsien RW. Proc. Natl. Acad. Sci. U.S.A. 2005; 102:2590–2595. [PubMed: 15699344]
7. Boland LM, Morrill JA, Bean BP. J. Neurosci. 1994; 14:5011–5027. [PubMed: 8046465]
8. Randall A, Tsien RW. J. Neurosci. 1995; 15:2995–3012. [PubMed: 7722641]
9. Stanley EF. Trends Neurosci. 1997; 20:404–409. [PubMed: 9292969]
10. Bucurenciu I, Bischofberger J, Jonas P. Nat. Neurosci. 2010; 13:19–21. [PubMed: 20010820]
11. Eggermann E, Bucurenciu I, Goswami SP, Jonas P. Nat Rev Neurosci. 2012; 13:7–21. [PubMed: 22183436]
12. Mintz IM, Sabatini BL, Regehr WG. Neuron. 1995; 15:675–688. [PubMed: 7546746]
13. Sidach SS, Mintz IM. J. Neurosci. 2000; 20:7174–7182. [PubMed: 11007873]
14. Neher E, Sakaba T. Neuron. 2008; 59:861–872. [PubMed: 18817727]
15. Navedo MF, et al. Circ. Res. 2010; 106:748–756. [PubMed: 20110531]
16. Phillips CG, Harnett MT, Chen W, Smith SM. J. Neurosci. 2008; 28:12062–12070. [PubMed: 19005071]
17. Hughes D, McBurney RN, Smith SM, Zorec R. J. Physiol. 1987; 392:231–251. [PubMed: 2451722]

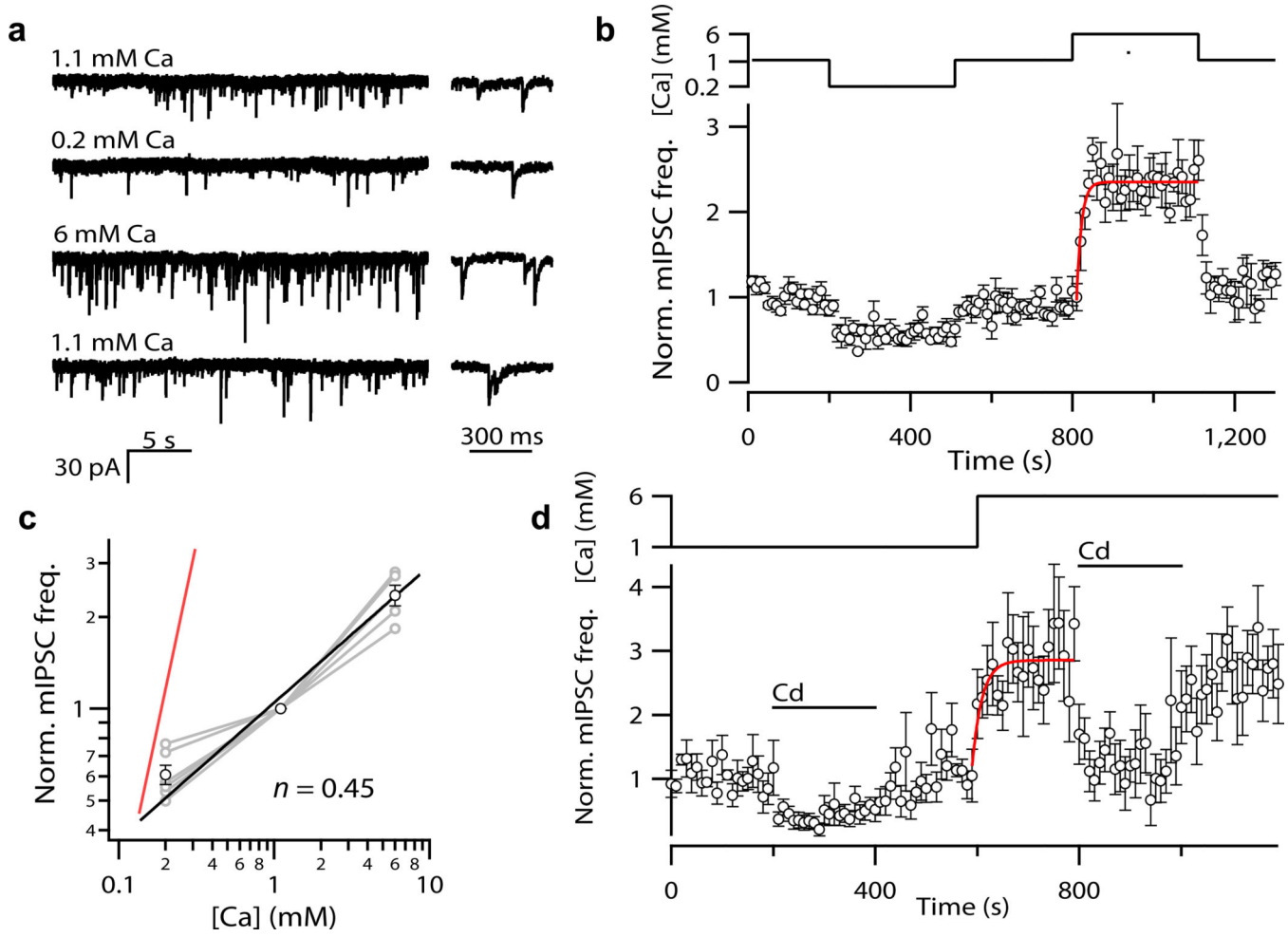

Figure 1.

VACCs mediate Ca^{2+}-dependent increases in mIPSC frequency. a, exemplary traces of mIPSCs at 0.2, 1.1 and 6 mM $[Ca^{2+}]_o$. Insets show expanded timescales. b, Average normalized plot of mIPSC frequency versus time (±SEM in this and subsequent figures; n=6). Response to increased $[Ca^{2+}]_o$ was well described by an exponential function (red curve, tau=12 s). c, log-log plot of the concentration-effect relationship for normalized mIPSC frequency versus $[Ca^{2+}]_o$. Responses from individual neurons are indicated in gray (n=6) and mean values are plotted in black. The data were fit with a line which had a slope of 0.45. A line with slope of 4 is shown in red for comparison[5]. d, Cd^{2+} reversibly reduces mIPSC frequency at physiological and elevated $[Ca^{2+}]_o$ in this average plot of normalized mIPSC frequency versus time (n=6). Response to increased $[Ca^{2+}]_o$ was described by an exponential function (tau=19 s).

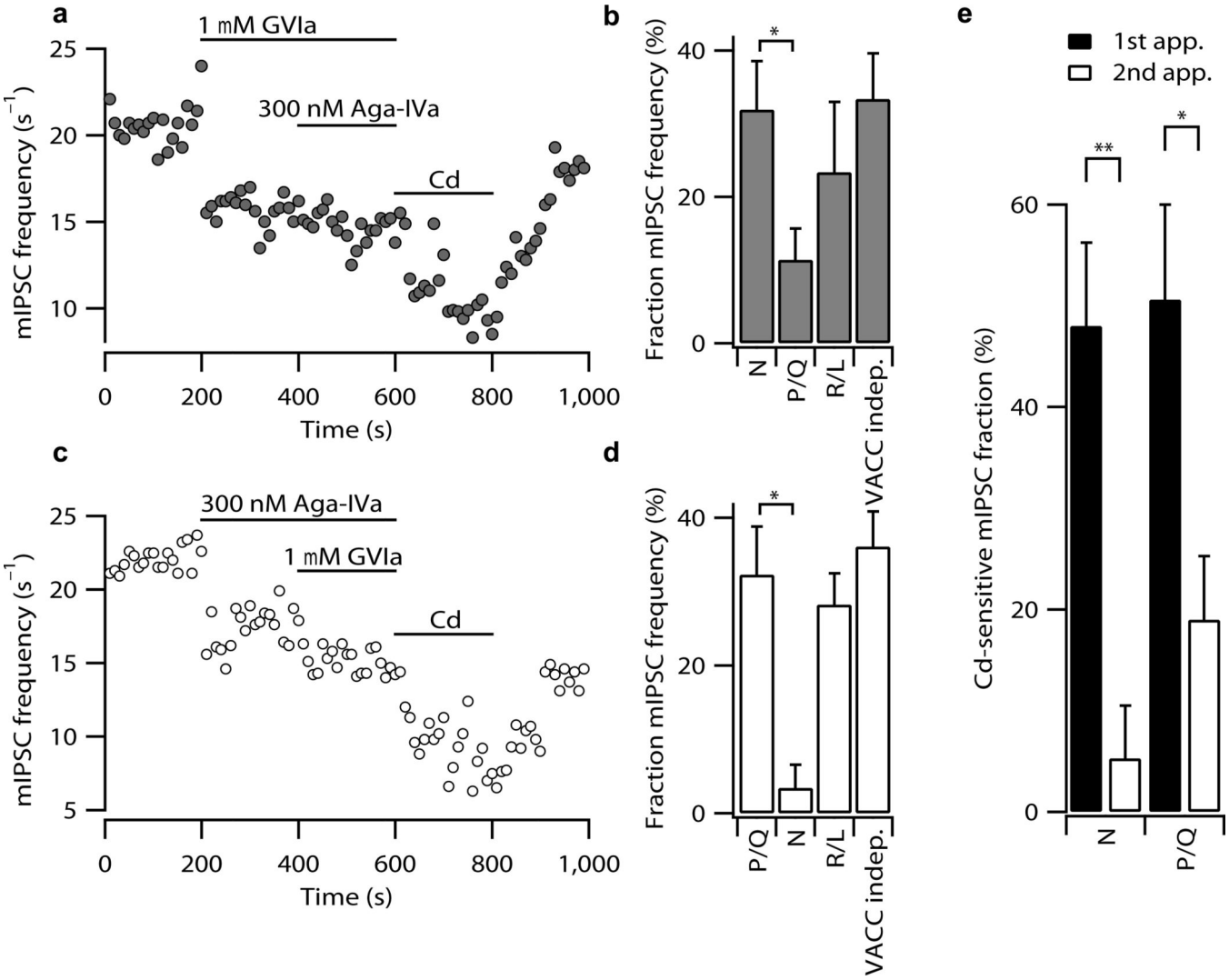

Figure 2.

Pharmacological dissection of the identity of VACCs mediating spontaneous GABA release. a, plot of mIPSC frequency versus time from an exemplary experiment indicating effects of GVIa, Aga-IVa, and Cd^{2+} in this order (at 1 μM, 300 nM, and 100 μM respectively in this and all other experiments). b, histogram indicating average effects on mIPSC frequency of these blockers when applied sequentially. c, plot of mIPSC frequency versus time from an exemplary experiment indicating effects of Aga-IVa, GVIa, and Cd^{2+} in this order. d, histogram indicating average effects on normalized mIPSC frequency of application of Aga-IVa, GVIa, and Cd^{2+}. e, effect of varying the order of application of Aga-IVa and GVIa on the Cd^{2+}-sensitive fraction of mIPSC frequency. The second application was always in the presence of a saturating dose the other blocker at steady state. Frequency of mIPSCs were reduced differently by first (filled bars) and second (open) applications of GVIa (48±8% vs 5±5%, n=9 vs 4; p=0.008) and Aga-IVa (51±9% vs 19±6%, n=4 vs 9; p=0.018). Here and in subsequent figures * and ** describe p-values of ≤0.05 and <l0.01.

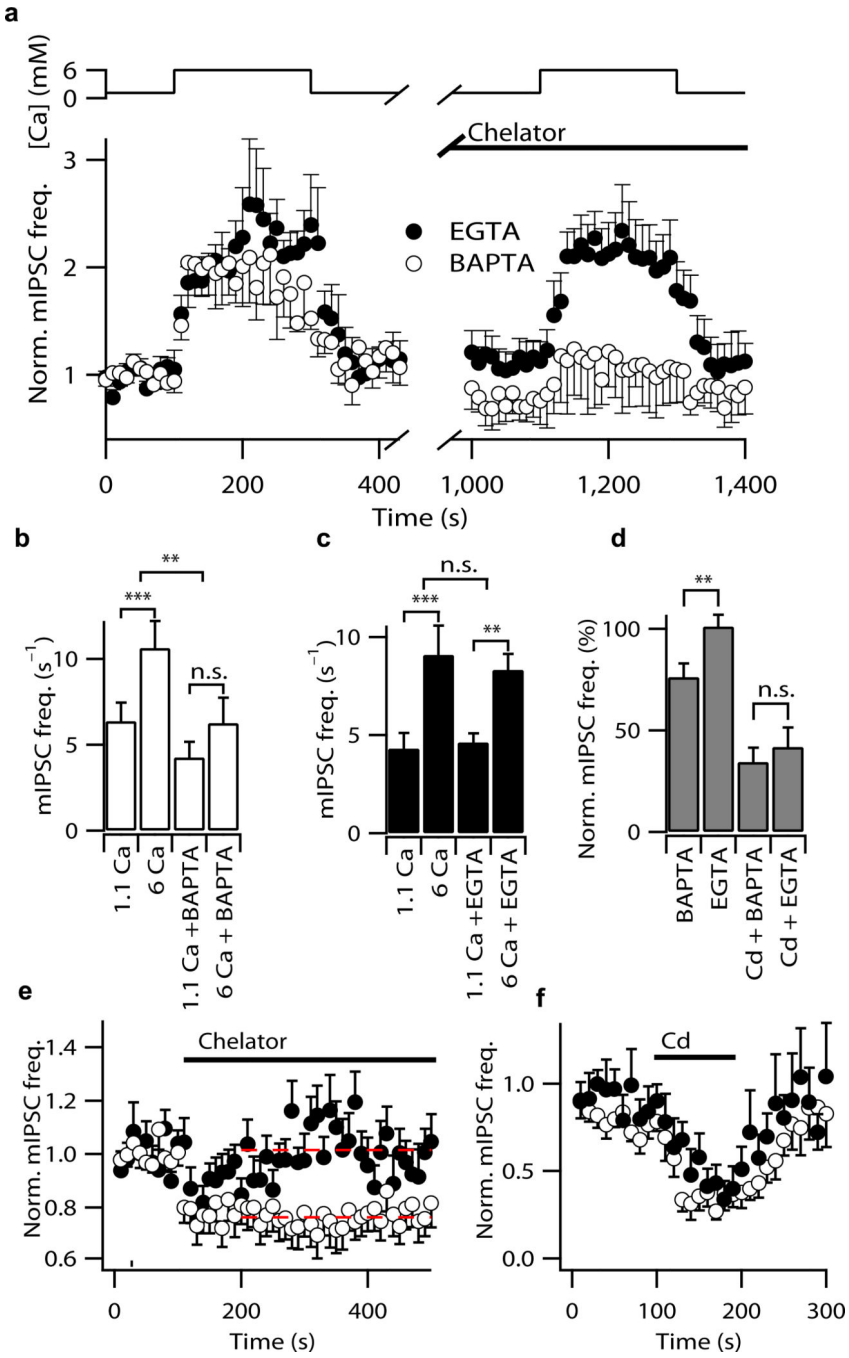

Figure 3.

VACC-vesicle coupling is attenuated by BAPTA-AM but not EGTA-AM. a, application of 50 μM BAPTA-AM (open circles, n=9), but not 50 μM EGTA-AM (filled, n=6), decreases the response to 6 mM Ca^{2+} in this plot of normalized average mIPSC frequency versus time. The thick black line indicates chelator application. b, c, histograms of steady-state mIPSC frequency from the same experiments as a in 1.1 or 6 mM $[Ca^{2+}]_o$ and in the absence and presence of BAPTA-AM (b, open bars) or EGTA-AM (c, filled). Here *** describes p-values <0.001.

d, histogram of normalized steady-state mIPSC frequency (200–500 s) in either BAPTA-AM (50 μM, n=14) or EGTA-AM (50 μM, n=17; left hand columns). Cd^{2+} inhibition of the mIPSC frequency following BAPTA-AM (n=7) or EGTA-AM (n=7) exposure is illustrated in the right hand columns. e, plot of normalized average mIPSC frequency versus time from the same experiments in d showing the affect of BAPTA-AM (open circles) and EGTA-AM (filled) on basal mIPSC frequency. Broken red lines indicate the average mIPSC frequency after 100s of chelator application. f, plot of normalized average mIPSC frequency showing the action of Cd^{2+} after 400s of chelator application for the same experiments as in e.